Monthly Notices of the ROYAL ASTRONOMICAL SOCIETY

Mon. Not. R. Astron. Soc. **399,** 2139–2145 (2009) doi:10.1111/j.1365-2966.2009.15414.x

The ongoing 2008–09 outburst of CI Cyg

A. Siviero,[1,2]★ U. Munari,[1] S. Dallaporta,[3] P. Valisa,[3] V. Luppi,[3] S. Moretti,[3] S. Tomaselli,[3] S. Bacci,[3] F. Ballardini,[3] G. Cherini,[3] M. Graziani,[3] A. Frigo[3] and A. Vagnozzi[3]

[1]*INAF Astronomical Observatory of Padova, 36012 Asiago (VI), Italy*
[2]*Astrophysikalisches Institut Potsdam, Potsdam, Germany*
[3]*ANS Collaboration, c/o Osservatorio Astronomico, via dell'Osservatorio 8, 36012 Asiago (VI), Italy*

Accepted 2009 July 17. Received 2009 July 17; in original form 2009 July 1

ABSTRACT

In this paper, we discuss the early phases of the ongoing outburst that CI Cyg, a prototype symbiotic star, is currently undergoing after 30-year quiescence. We have tightly monitored CI Cyg in $BVR_{\rm C}I_{\rm C}$ bands, starting a whole year before the onset of the outburst, and in addition we obtained numerous Echelle high- and low-resolution absolutely flux-calibrated spectra. The outburst started while the accreting white dwarf (WD) was being eclipsed by the Roche lobe filling M giant companion, and it was discovered during the egress phase on the second half of 2008 August. The system reached peak V-band brightness in early 2008 October and has been characterized by amplitudes $\Delta B = 1.9$, $\Delta V = 1.5$, $\Delta R_{\rm C} = 0.9$, $\Delta I_{\rm C} = 0.4$ mag. At maximum V-band brightness, the outbursting WD had expanded to closely resemble an F3 II/Ib star, with $M_V = -3.5$, $T_{\rm eff} \sim 6900$ K and $R = 28\,{\rm R}_{\odot}$. The high-ionization emission lines ([Ne V], [Fe VII], He II) disappeared and only lower ionization lines were visible. Balmer and He I emission lines declined in equivalent width but increased in absolute flux. The output radiated by the hot component during the outburst corresponds to nuclear burning proceeding at a $2 \times 10^{-8}\,{\rm M}_{\odot}\,{\rm yr}^{-1}$ rate.

Key words: binaries: symbiotic – novae, cataclysmic variables.

1 INTRODUCTION

CI Cyg is a prototype symbiotic star, and one of the first discovered (Shapley 1922; Merrill & Humason 1932). It hosts an M5.5 giant star (Mürset & Schmid 1999), with no significant circumstellar dust. It shows a marked ellipsoidal effect in its long-wavelength light curves (Mikołajewska et al. 2003) indicating that the giant component is filling, or nearly filling, its tidal Roche lobe. The mass transfer from the giant to the hot component should therefore mainly occur via Roche lobe overflow.

The nature of the accreting compact star in CI Cyg is still controversial. Kenyon et al. (1991, hereafter K91) argued from ultraviolet (UV) colours that the hot source should be a $0.5\,{\rm M}_{\odot}$ main-sequence star, surrounded by an extended disc, accreting at $\dot{M} \approx 1$–$3 \times 10^{-5}\,{\rm M}_{\odot}\,{\rm yr}^{-1}$. Godon (1996) derived $T_{\rm bl} = 120\,000$ K as the temperature of the boundary layer of the disc around a 0.5 $\rm M_{\odot}$, 0.2 $\rm R_{\odot}$ star accreting at this rate. The high temperature would account for the high-ionization emission lines (He II, [Ne V] and [Fe VII]) observed in CI Cyg during quiescent states. However, a disc around a main-sequence star would not be able to account for the outburst states of CI Cyg. Godon's models show that the only way to account for the much lower temperatures observed during outburst ($T \le 20\,000$ K) is to invoke a large expansion ($\geq$2) in the radius of the accreting star. Playing with the accretion rate would not produce the desired effect.

Tutukov & Yungelson (1976) and Paczynski & Rudak (1980) proposed that a good fraction of known symbiotic stars were powered by stable hydrogen nuclear burning, on the surface of a white dwarf, of the material accreted from the cool giant companion. This was confirmed observationally by Munari & Buson (1994), and later by Sokoloski (2003). The conditions for stable H-burning and smallest envelope radius (e.g. maximum temperature of the pseudo-photosphere) require a fine-tuning of the mass accretion rate (cf. Kenyon 1986, hereafter K86, and references therein). The burning envelope would react with an expansion (and consequent cooling of the pseudo-photosphere) to any increase of the accretion rate above the minimum amount required to sustain stable nuclear burning. Should this occur, the pseudo-photosphere would shift its energy peak from far-UV into the optical range, causing the star to appear in 'outburst'. The increase of the accretion rate on to the WD could be triggered by enhanced mass loss from the cool giant or by mass dump through an accretion disc (e.g. Sokoloski et al. 2006). Mikołajewska (2003) argued that the collected observational facts

★E-mail: alessandro.siviero@oapd.inaf.it

suggest abandoning the K91 model for CI Cyg of a main-sequence star accretor in favour of a WD in stable H-burning conditions at the surface.

CI Cyg has experienced only a few outbursts in its long recorded history (K86 and references therein). Those of 1911 and 1937 have been quite minor ones, in both brightness amplitude and duration. Then, between 1970 and 1978, CI Cyg experienced a major outburst phase, characterized by several brightness maxima peaking at $V \leq$ 9.0 mag and year-long declines, interspersed by total eclipses of the outbursting WD by the cool giant (e.g. Belyakina 1979, 1984). Following it, CI Cyg experienced 30 years of flat quiescence, until when in 2008 we discovered it again in outburst (Munari et al. 2008). The current outburst is far brighter and longer in duration that the 1911 and 1937 events, and it is so far comparable to the early development of the 1970–1978 outburst. Being the first such event since the introduction of linear detectors (CCDs) in Astronomy, it will offer the unprecedented opportunity for a throughout study of CI Cyg. In this paper, we report about the early development of the outburst as resulting from our all-out observational effort based on BVR_CI_C photometry, wide wavelength range absolute spectrophotometry and high-resolution spectroscopy.

2 OBSERVATIONS

CCD observations of CI Cyg in the BVR_CI_C bands were obtained with the following Asiago Novae and Symbiotic Stars (ANS) Collaboration[1] telescopes in Italy, identified in this paper by their code: (R010) – a 0.13-m f/6.6 Vixen ED130SS refractor in Trieste; (R030) – the 0.30-m Meade RCX-400 f/8 Schmidt–Cassegrain of Associazione Astrofili Valle di Cembra (Trento); (R071) – a 0.40-m Meade LX200 telescope in Catania; (R120) – the 0.42-m f/5.4 Newton telescope operated in Bastia (Ravenna) by Associazione Ravennate Astrofili Rheyta; (R130) – the 0.50-m f/6 Ritchey-Cretien telescope of Associazione Ternana Astrofili (Stroncone, Terni). All observations have been fluxed and colour-corrected using the Henden & Munari (2006) $UBVR_CI_C$ photometric comparison sequence around CI Cyg. Our data are plotted in Fig. 1 and presented in Table 1. The quoted errors quadratically include both the Poissonian component and the uncertainty of the colour equation transformation.

High- and low-resolution spectra of CI Cyg were obtained with different instruments in Italy, all adopting a 2.0 arcsec wide slit, east–west oriented. A journal of observation is given in Table 2. We used (i) the 0.60-m telescope of Osservatorio Astronomico G. Schiapparelli (Campo dei Fiori, Varese), equipped with a multimode spectrograph (MMS) housing on a turnable optical bench both an Echelle instrument as well as various single-dispersion combinations; (ii) the 1.82-m telescope operated in Asiago by the National Institute for Astrophysics (INAF) Astronomical Observatory of Padova, equipped with both single-dispersion and Echelle grating spectrographs; (iii) the 1.22-m telescope of the Asiago Astrophysical Observatory of the University of Padova and a Boller & Chivens single-dispersion grating spectrograph. All spectra have been extracted and calibrated for bias, dark, flat and spectrophotometric standards with IRAF. Integrating the BVR_C photometric passbands over the single-dispersion spectra provides values coincident within 0.1 mag of the CCD photometry of Table 3 and Fig. 1. The accuracy of the wavelength scale of the Echelle spectra is always better than 1.2 km s^{-1} as derived by measurement of the night-sky and city-light emission lines as well as the telluric O_2 and H_2O absorption lines.

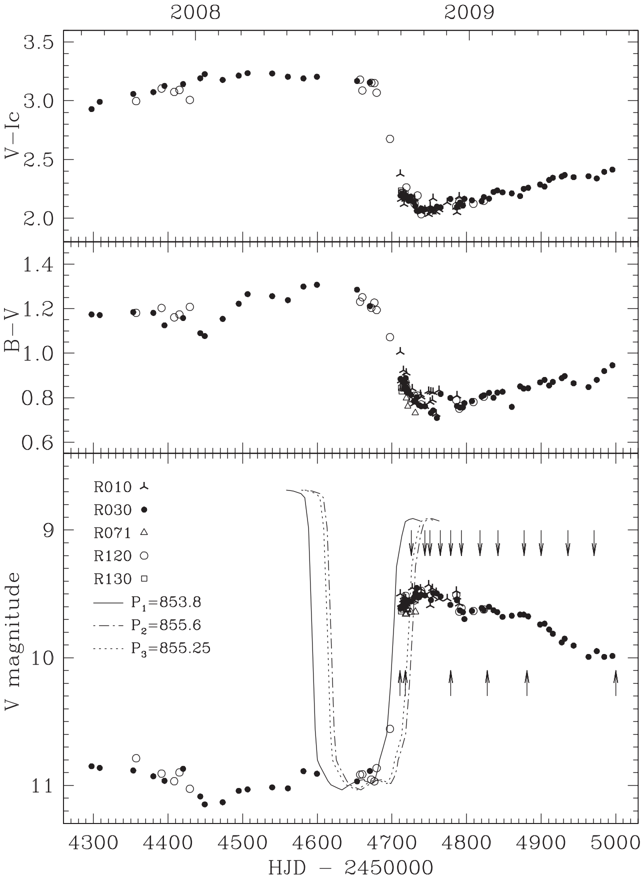

Figure 1. Light curves of CI Cyg from our CCD observations. Upward and downward arrows mark the time of Echelle and low-resolution spectroscopic observations, respectively (cf. Table 2).

3 THE OUTBURST

The photometric evolution of CI Cyg, over the last 600 days, is presented in Fig. 1. It is characterized by the star remaining at brightness and colour levels typical of quiescence until early 2008 August. Then, on August 18 we detected CI Cyg abnormally bright at $V = 10.55$, and when we re-observed it at $V = 9.55$ on August 31, it was clear that the object was entering an outburst phase, the first after 30 years of flat quiescence. The actual onset of the outburst has been probably missed, because right at that time CI Cyg was undergoing an eclipse of the hot component by the cool giant companion. When CI Cyg re-emerged from the eclipse, the hot component was already in outburst. In Fig. 1, we have plotted the V-band profile of the 1975 eclipse (occurring during the brightest peak of the multimaxima 1970–1978 outburst phase) obtained by the data from Belyakina (1984). The 1975 eclipse profile has been plotted in Fig. 1 following three different orbital periods given in the literature for CI Cyg. The 855.6 days proposed by Mikołajewska (1997, dot–dashed line in Fig. 1), and the 855.25 days by Mikołajewska & Mikolajewski (1983, dotted line), provide results in conflict with the 2008 observations, while there is a good agreement with the 853.8 days derived spectroscopically by Fekel et al. (2000,

[1] The ANS Collaboration is an Italian network of amatorial and professional telescopes supervised by the Asiago Observatory. More about the project will be presented in a forthcoming paper.

Table 1. BVR_CI_C photometry of CI Cyg.

HJD	V	ϵ_V	$B-V$	ϵ_{B-V}	$V-R_C$	ϵ_{V-R}	$V-I_C$	ϵ_{V-I}	Observation
4297.5199	10.850	0.008	1.174	0.008	0.914	0.009	2.929	0.026	R030
4308.4743	10.863	0.002	1.171	0.007	0.957	0.016	2.991	0.047	R030
4353.4444	10.883	0.003	1.184	0.003	0.865	0.008	3.058	0.006	R030
4357.3119	10.787	0.004	1.181	0.007	0.686	0.010	2.997	0.007	R120
4380.3345	10.928	0.004	1.181	0.004			3.073	0.007	R030
4391.3581	10.907	0.003	1.203	0.003	1.239	0.010	3.104	0.009	R120
4395.3054	10.964	0.003	1.125	0.006			3.126	0.004	R030
4408.3141	10.967	0.002	1.161	0.004	1.598	0.018	3.075	0.005	R120
4415.2961	10.898	0.004	1.174	0.004	1.534	0.005	3.092	0.005	R120
4420.2520	10.870	0.005	1.158	0.019			3.142	0.008	R030
4429.2880	11.026	0.006	1.208	0.005	1.526	0.004	3.007	0.007	R120
4443.2292	11.086	0.003	1.090	0.012			3.191	0.011	R030
4449.2440	11.148	0.006	1.077	0.015			3.226	0.011	R030
4473.2304	11.132	0.009	1.154	0.027			3.177	0.019	R030
4494.7020	11.042	0.006	1.222	0.019			3.214	0.011	R030
4506.6880	11.031	0.006	1.265	0.007			3.235	0.005	R030
4539.6182	11.015	0.008	1.256	0.022			3.232	0.014	R030
4560.6115	11.023	0.011	1.238	0.012			3.204	0.008	R030
4581.4904	10.888	0.002	1.299	0.016			3.190	0.009	R030
4599.5829	10.908	0.004	1.307	0.012			3.204	0.009	R030
4653.3503	10.968	0.004	1.285	0.017			3.168	0.010	R030
4657.4288	10.915	0.008	1.231	0.022	1.271	0.009	3.180	0.030	R120
4660.4475	10.913	0.011	1.251	0.015	1.625	0.011	3.087	0.015	R120
4670.4720	10.887	0.003	1.211	0.008			3.156	0.011	R030
4672.4368	10.954	0.009	1.204	0.022	1.550	0.020	3.153	0.016	R120
4676.5167	10.968	0.014	1.227	0.019	1.673	0.017	3.150	0.016	R120
4679.5568	10.864	0.013	1.194	0.014	1.701	0.032	3.069	0.012	R120
4697.4522	10.557	0.017	1.072	0.042	1.595	0.026	2.676	0.013	R120
4711.3776	9.499	0.052	1.006	0.051	0.792	0.156	2.378	0.114	R010
4711.5480	9.613	0.004	0.884	0.010			2.193	0.007	R030
4712.3134	9.638	0.001	0.844	0.007	0.919	0.006	2.236	0.009	R130
4712.3719	9.579	0.002	0.877	0.026	0.861	0.027	2.163	0.013	R010
4713.3032	9.610	0.001	0.828	0.007	0.902	0.007	2.219	0.006	R130
4714.2851	9.601	0.006	0.871	0.006			2.207	0.005	R030
4714.3061	9.622	0.001	0.850	0.008	0.912	0.005	2.223	0.007	R130
4715.2947	9.598	0.001	0.841	0.006	0.891	0.005	2.210	0.007	R130
4715.3736	9.544	0.004	0.923	0.039	0.902	0.021	2.204	0.021	R010
4715.6108	9.581	0.010					2.173	0.017	R030
4716.2846	9.575	0.005	0.842	0.013					R030
4716.4078	9.521	0.005	0.892	0.025	0.856	0.072	2.120	0.036	R010
4717.3630	9.541	0.007	0.869	0.006			2.187	0.006	R030
4718.3097	9.594	0.002	0.854	0.006	0.903	0.008	2.209	0.008	R130
4718.3318	9.515	0.007	0.869	0.023	1.412	0.037	1.005	0.026	R120
4718.3502	9.537	0.007	0.877	0.016	0.879	0.036	2.163	0.033	R010
4718.4585	9.658	0.010	0.847	0.049					R071
4718.5084	9.598	0.004	0.888	0.009			2.195	0.007	R030
4719.3527	9.608	0.009	0.847	0.030	1.040	0.023	2.263	0.031	R120
4719.3546	9.575	0.003	0.912	0.042	0.861	0.019	2.199	0.012	R010
4719.4759	9.656	0.010	0.798	0.157					R071
4719.4859	9.579	0.005	0.846	0.016			2.179	0.010	R030
4720.4011	9.620	0.005	0.836	0.068					R071
4720.4104	9.568	0.005	0.823	0.016			2.182	0.013	R030
4721.3641	9.626	0.009	0.762	0.094					R071
4722.3886	9.552	0.003	0.829	0.013			2.149	0.008	R030
4725.4021	9.643	0.005	0.790	0.009					R071
4725.4246	9.559	0.006	0.813	0.023			2.185	0.008	R030
4727.3249	9.452	0.005	0.841	0.048	0.773	0.034	2.150	0.022	R010
4727.3835	9.547	0.002	0.794	0.010	0.871	0.008	2.169	0.011	R130
4729.4527	9.528	0.004	0.785	0.016			2.138	0.008	R030
4730.3425	9.551	0.012	0.809	0.030	1.089	0.034	2.125	0.021	R120
4730.3499	9.553	0.003	0.774	0.042	0.889	0.035	2.169	0.009	R010
4731.4115	9.640	0.026	0.732	0.196					R071
4731.5028	9.495	0.004	0.783	0.012			2.103	0.016	R030

Table 1 – *continued*

HJD	V	ϵ_V	$B-V$	ϵ_{B-V}	$V-R_C$	ϵ_{V-R}	$V-I_C$	ϵ_{V-I}	Observation
4733.2737	9.453	0.002	0.802	0.007			2.064	0.008	R030
4734.3979	9.519	0.014	0.810	0.048	1.053	0.030	2.194	0.026	R120
4736.2792	9.527	0.004	0.767	0.014			2.063	0.012	R030
4738.2949	9.460	0.009	0.815	0.038	0.779	0.039	2.070	0.026	R010
4739.2899	9.510	0.004	0.762	0.025			2.084	0.017	R030
4739.3051	9.476	0.019	0.770	0.028	1.062	0.032	2.035	0.020	R120
4739.3092	9.486	0.004	0.805	0.020	0.779	0.015	2.054	0.025	R010
4744.2883	9.511	0.003	0.762	0.027	0.835	0.026	2.074	0.011	R010
4744.3691	9.512	0.005	0.762	0.021			2.077	0.007	R030
4749.3767	9.429	0.005	0.830	0.009	0.782	0.030	2.034	0.024	R010
4751.2764	9.590	0.004	0.781	0.024	0.832	0.018	2.106	0.015	R010
4752.2784	9.480	0.005	0.827	0.046	0.777	0.041	2.057	0.050	R010
4752.3475	9.548	0.004	0.732	0.011			2.083	0.008	R030
4754.2613	9.457	0.007	0.790	0.036	0.777	0.042	2.056	0.024	R010
4755.2613	9.520	0.018	0.825	0.042	0.825	0.031	2.170	0.027	R010
4755.3046	9.494	0.003	0.743	0.028			2.076	0.014	R030
4759.2724	9.487	0.004	0.727	0.010	0.820	0.033	2.054	0.009	R010
4760.2528	9.496	0.004	0.709	0.013			2.099	0.011	R030
4763.2813	9.539	0.006	0.834	0.016	0.848	0.022	2.076	0.031	R010
4765.2935	9.520	0.005	0.817	0.008			2.093	0.006	R030
4774.2501	9.537	0.002			0.840	0.042	2.135	0.026	R010
4778.3720	9.586	0.012	0.799	0.026			2.164	0.007	R030
4786.2861	9.508	0.008	0.789	0.022	0.955	0.039	2.103	0.022	R120
4786.3245	9.477	0.005			0.781	0.059	2.097	0.036	R010
4787.2350	9.550	0.003	0.763	0.007			2.097	0.009	R030
4787.2493	9.522	0.003	0.809	0.011	0.828	0.040	2.050	0.015	R010
4790.3268	9.577	0.010			0.808	0.059	2.185	0.048	R010
4790.3329	9.639	0.004	0.751	0.008	1.013	0.032	2.141	0.013	R120
4791.2647	9.630	0.006	0.756	0.013			2.134	0.013	R030
4793.2262	9.610	0.003	0.763	0.010	1.035	0.017	2.118	0.014	R120
4795.2432	9.643	0.004	0.757	0.011			2.109	0.009	R030
4797.1947	9.697	0.007	0.776	0.022			2.166	0.008	R030
4807.3333	9.633	0.007	0.785	0.014			2.153	0.011	R030
4809.2551	9.634	0.005	0.781	0.028	1.004	0.009	2.124	0.017	R120
4820.2271	9.611	0.005	0.805	0.020			2.145	0.008	R030
4823.2297	9.625	0.009	0.811	0.018			2.181	0.009	R030
4823.2334	9.622	0.004	0.805	0.009	1.020	0.015	2.149	0.018	R120
4830.2391	9.601	0.002	0.822	0.023			2.167	0.013	R030
4836.2033	9.628	0.002	0.800	0.033			2.224	0.016	R030
4841.2491	9.643	0.006	0.823	0.013			2.237	0.014	R030
4848.2313	9.680	0.005	0.827	0.010			2.221	0.007	R030
4860.6897	9.671	0.006	0.759	0.019			2.212	0.013	R030
4871.7297	9.662	0.005	0.851	0.048			2.189	0.011	R030
4876.6523	9.662	0.005	0.841	0.008			2.250	0.009	R030
4882.6475	9.676	0.005	0.843	0.010			2.26	0.011	R030
4898.6097	9.740	0.005	0.869	0.010			2.287	0.018	R030
4904.6091	9.733	0.009	0.880	0.020			2.270	0.017	R030
4910.6480	9.779	0.006	0.855	0.008			2.326	0.013	R030
4915.6389	9.812	0.005	0.871	0.011			2.345	0.012	R030
4927.5673	9.880	0.004	0.888	0.007			2.356	0.011	R030
4931.5729	9.851	0.005	0.897	0.014			2.368	0.012	R030
4943.4915	9.905	0.005	0.865	0.016			2.350	0.016	R030
4963.4291	9.993	0.005	0.848	0.012			2.358	0.009	R030
4974.4989	9.948	0.002	0.880	0.009			2.339	0.006	R030
4984.5297	9.993	0.005	0.920	0.014			2.395	0.008	R030
4995.5002	9.986	0.005	0.946	0.013			2.414	0.012	R030

hereafter F00, solid line). The orbital ephemeris is therefore

$$\mathrm{Min}(V) = 2442\,690 + 853.8E, \quad (1)$$

where the epoch is the photocentre of the 1975 eclipse.

In quiescence (cf. the spectra for 1995 and 2003 in Fig. 2), the optical spectrum of CI Cyg was dominated by the molecular absorptions of the cool giant and by high-ionization emission lines ([Ne V], [Fe VII], He II) powered by the very hot WD companion. During the 2008 outburst, the temperature of the hot companion

Table 2. Journal of the spectroscopic observation. The fourth column lists the resolving power (in slanted characters) for the Echelle spectrographs and dispersion (in Å pixel^{-1}) for the others.

Date	UT	Expt. (s)	Disp. (Å pixel^{-1})	Telescope
1994-11-13	20:03	240	*17 000*	ECH 1.82-m
1995-10-14	22:05	140	7.7	B&C 1.82-m
2003-08-09	24:16	2760	7.7	B&C 1.22-m
2008-09-01	20:04	2400	1.8	MMS 0.60-m
2008-09-08	19:22	1320	2.3	B&C 1.22-m
2008-09-16	21:42	5400	*11 000*	ECH 0.60-m
2008-10-04	20:58	5400	*11 000*	ECH 0.60-m
2008-10-11	21:45	5400	*11 000*	ECH 0.60-m
2008-10-25	22:35	4500	*11 000*	ECH 0.60-m
2008-11-08	18:38	3000	1.8	MMS 0.60-m
2008-11-08	20:49	5400	*11 000*	ECH 0.60-m
2008-11-22	20:30	5400	*11 000*	ECH 0.60-m
2008-12-17	19:35	5400	*11 000*	ECH 0.60-m
2008-12-27	18:28	2700	1.8	MMS 0.60-m
2009-01-10	17:42	4500	*11 000*	ECH 0.60-m
2009-02-15	04:00	3600	*11 000*	ECH 0.60-m
2009-02-19	04:12	2700	1.8	MMS 0.60-m
2009-03-10	04:02	3600	*11 000*	ECH 0.60-m
2009-04-15	01:12	4500	*11 000*	ECH 0.60-m
2009-05-19	22:22	3600	*11 000*	ECH 0.60-m
2009-06-17	25:48	1200	2.3	B&C 1.22-m

greatly decreased (all high-ionization emission lines disappeared) and the peak of its energy distribution shifted from the UV into the optical wavelength range, overwhelming the absorption spectrum of the cool giant. Only low-ionization emission lines were visible at maximum optical brightness (see Fig. 2), most notably Balmer,

Table 3. Integrated absolute fluxes (in erg cm^{-2} s^{-1}) and equivalent widths (in Å) of Hβ, He I 5876 and Hα emission lines in the spectra of Fig. 2. The 'quiescence' values are obtained by averaging together K91 1981–88 data and 1995 and 2003 spectra in Fig. 2.

	Hβ		He I 5876		Hα	
	Flux	EW	Flux	EW	Flux	EW
Quiescence	3.1E-12	55	1.7E-12	15	5.4E-11	210
2008-09-01	9.3E-12	30	4.4E-12	10	1.2E-10	174
2008-09-08	1.5E-11	36	4.7E-12	9	1.3E-10	164
2008-11-08	1.7E-11	39	4.2E-12	9	1.4E-10	184
2008-12-27	2.4E-11	37	6.0E-12	9	1.5E-10	181
2009-02-19	1.6E-11	45	5.2E-12	11	1.4E-10	187
2009-06-17	1.8E-11	68	5.4E-12	18	1.2E-10	273

He I, Fe II multiplets 26, 27, 35, 37, 38, 40, 41, 42, 46, 48, 49, 55, 74, Si II multiplets 2, 4, 5 and [O I]. While the equivalent width of Balmer and He I lines decreased relative to quiescence because of the brightening underlying continuum, their absolute fluxes actually increased (cf. Table 4), reaching the peak absolute intensity on the 2008 December 27 spectrum. The more recent spectrum (2008 June 17; on the top of Fig. 2) has been acquired when the system was 0.5 V-band magnitude fainter than its 2008 October maximum (see below) and high-ionization emission lines (He II) start to reappear, indicating that the pseudo-photosphere of the expanded WD is retracting and warming.

Maximum V-band brightness was reached at 9.50 ± 0.01 mag during the first week of 2008 October, with colours $B - V = +0.78 \pm 0.01$, $V - R_{\rm C} = +0.80 \pm 0.01$, $V - I_{\rm C} = +2.07 \pm 0.01$. The multi-epoch photometric catalogue of symbiotic stars of Henden & Munari (2008) reports for CI Cyg in quiescence during

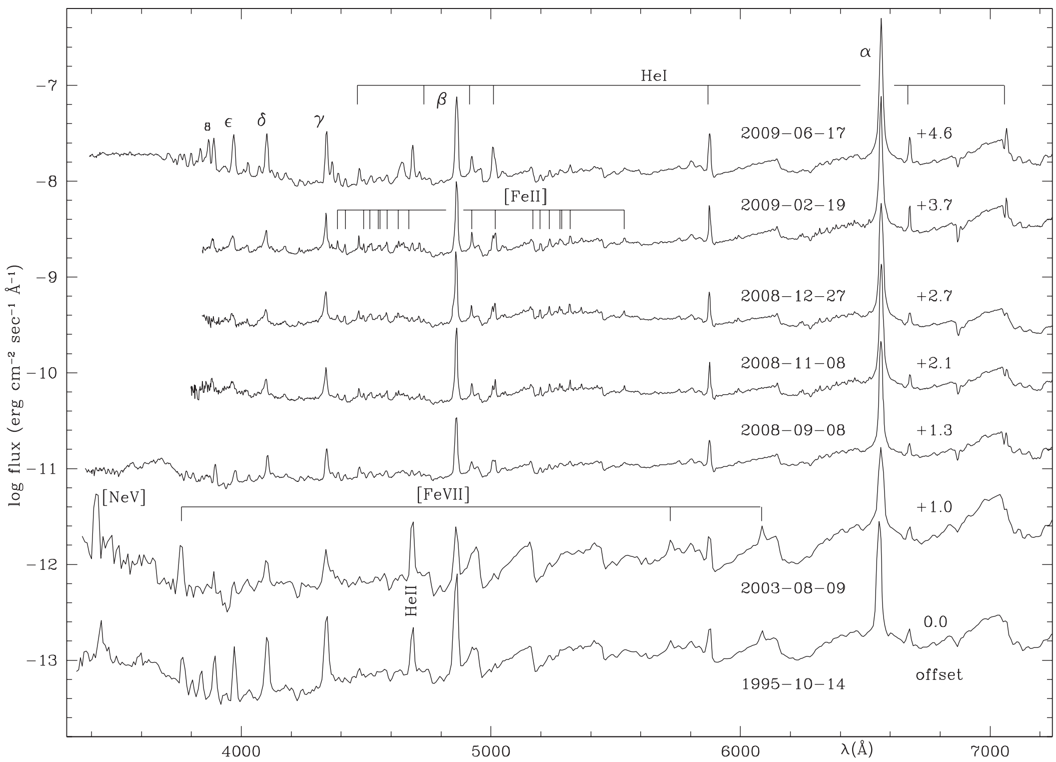

Figure 2. Low-resolution spectral evolution of CI Cyg during the early development of the 2008 outburst. The quiescence spectra for 1995 and 2003 are given for comparison. For clarity, the spectra are offset in ordinates by the quantity given on the right.

Table 4. Radial velocity (in km s^{-1}), standard deviation (σ, in km s^{-1}) and integrated flux (in 10^{-11} erg cm^{-2} s^{-1}) of the four Gaussian components used to fit the high-resolution Hα profiles presented in Fig. 3. The radial velocity of the M giant is from the orbit of F00. That for the WD is for a mass ratio 3 (from K91) and a systemic velocity of 15 km s^{-1} (from F00, final solution).

Date	Orbital	Emission			Absorption			Pedestal			Bump			M giant	WD	He II
	phase	*rv*	σ	flux	*rv*	σ	flux	*rv*	σ	flux	*rv*	σ	flux	*rv*	*rv*	*rv*
2008-09-16	0.097	+5	70	15.90	−9	33	−7.19	+30	300	3.93	−300	120	0.37	19.9	0.3	−9
2008-10-04	0.118	+0	72	15.53	−12	33	−6.48	+40	320	3.49	−310	120	0.76	20.6	−1.8	−12
2008-10-11	0.127	+3	72	14.74	−7	30	−6.11	+40	300	4.47	−280	120	0.50	20.9	−2.7	−13
2008-10-25	0.143	+3	64	14.71	−8	32	−7.32	−15	280	5.94	+230	100	0.48	21.3	−3.9	−14
2008-11-08	0.159	+0	64	15.25	−8	32	−7.53	−20	280	5.89	+280	110	0.39	21.7	−5.1	−15
2008-11-22	0.176	+0	64	15.83	−9	30	−7.18	−20	250	5.51	+330	100	0.34	21.8	−5.4	−16
2008-12-17	0.205	+0	62	14.94	−7	30	−7.28	−25	240	6.82	+250	80	0.53	22.0	−6.0	−16
2009-01-10	0.233	+0	64	14.54	−8	29	−6.62	−20	250	5.78	+230	93	0.70	21.7	−5.1	−14
2009-02-15	0.274	+0	67	14.49	−10	29	−6.05	−23	250	5.14	+290	100	0.41	20.9	−2.7	−14
2009-03-10	0.301	−3	65	9.74	−12	30	−4.43	−23	250	3.51	+290	100	0.26	20.7	−2.1	−13
2009-04-15	0.344	−3	65	7.58	−16	31	−3.32	−5	250	2.74	+180	80	0.22	19.2	−2.4	−8
2009-05-19	0.384	−3	64	8.26	−15	33	−3.91	−15	220	2.58	+200	80	0.28	17.9	+6.3	−4
1994-11-13	0.175	−1	58	5.37	−12	34	−1.56							21.8	−5.4	−16

the summer of 2001 the mean colours: $V = 11.20$, $B - V = +1.44$, $V - R_C = +1.48$, $V - I_C = +3.28$. The mean values during the quiescence of Fig. 1 are $V = 10.95$, $B - V = +1.20$, $V - R_C = +1.33$, $V - I_C = +3.13$. If we assume that they trace the contribution of the cool giant and if we subtract them from the overall system flux, after correcting for $E_{B-V} = 0.45$ and scaling to a distance of $\sim$2.3 kpc (cf. K91), we obtain for the outbursting component at V-band maximum $M_V = -3.5$, $(B - V)_\circ = +0.25$, $(V - R_C)_\circ = +0.23$, $(V - I_C)_\circ = +0.52$. Even if the colour match that of classical novae at maximum [$(B - V)_\circ = +0.23 \pm 0.06$, van der Bergh & Younger 1987], the absolute magnitude is largely fainter than that of classical novae at 15 days past maximum ($M_V = -5.5$; Warner 1995), a value which is independent from nova type and speed class. Such a hot component has radiated $\sim 1 \times 10^{44}$ erg during the first 200 days of the outburst, corresponding to the nuclear burning at a rate $\sim 2 \times 10^{-8}$ M$_\odot$ yr^{-1} of material of solar composition. According to numerical values in K86, this is just slightly (approximately two times) above the accretion rate required for stable H burning on a WD of the mass (0.5 M$_\odot$) estimated by K91 for CI Cyg. This supports the idea that the WD in CI Cyg was burning hydrogen at its surface during quiescence and that the 'outburst' was triggered by an increase of the mass accretion rate above the stability threshold, causing the envelope around the WD to expand and cool in response.

Absolute magnitude and intrinsic colours nicely fit an F3 II/Ib classification for the WD at V-band maximum, to which would correspond an effective temperature $T_{\rm eff} \sim 6900$ K and a radius $R = 28$ R$_\odot$ (Straižys 1992; Drilling & Landolt 2000; Sowell et al. 2007). This radius is in excellent agreement with the value $R \sim 28$ R$_\odot$ resulting from the duration ($\sim$17 days) of egress from the eclipse coupled with F00 orbit and K91 mass ratio $\sim$3. The spectroscopic and photometric evolution of the 1970–1978 and current outbursts of CI Cyg is highly reminiscent of the similar train of several maxima and total eclipses characterizing the 1988–1996 outburst of the symbiotic star AS 296 (Munari et al. 1995).

The current outburst has reached the same brightness as the first maximum in the 1970–1978 event. It is therefore possible that CI Cyg has entered a new, long-lasting outburst phase similar to that of 30 years ago, with brighter maxima expected to occur over the coming few years. The next eclipse will run from the end of 2010 August (first contact) to early 2011 January (fourth contact), with totality lasting from about 2010 September 11 to December 16.

The evolution of the Hα emission profile during the current outburst is shown in Fig. 3 (where the orbital phases are computed according to equation 1). A fitting with a set of four Gaussians [one each for the main emission component (MEC), the sharp absorption, the wide pedestal and the bump] is overplotted as a dashed line, and their parameters are listed in Table 3. The profile is quite different from that in quiescence at similar orbital phases (see for comparison the 1994-10-13 profile at the top of Fig. 3). The

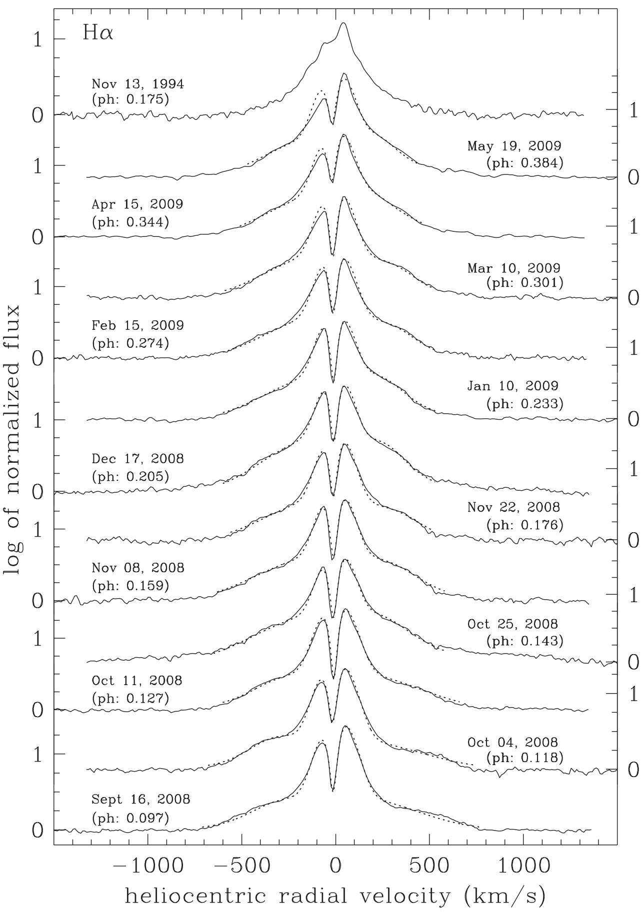

Figure 3. Evolution of the Hα profile during the 2008 outburst.

absorption component has become approximately five times stronger while keeping the same width and radial velocity of quiescence stable at about -25 km s^{-1} with respect to the barycentric velocity of the binary system ($+15$ km s^{-1} from F00). It traces external, neutral gas, expanding with the velocity expected for the wind of the cool giant, which is dynamically decoupled from the orbital motion and that therefore engulfs the whole binary system. The MEC increases its integrated flux by approximately three times in comparison to quiescence. After a small increase (20 per cent) in width at the onset of the outburst, the MEC has returned soon after maximum brightness to the narrow width observed in quiescence. A brand new component has appeared during the outburst, in the form of a wide pedestal, whose radial velocity seems to vary over a far wider interval than MEC. The integrated flux of the pedestal is about one-third of MEC and, similarly to the latter, the pedestal has reduced its width by 30 per cent along the monitored outburst evolution. Finally, a weak 'bump' component was fitted to the profile to account for an asymmetry in the Hα wings observed to travel from -310 to a maximum value of $+330$ km s^{-1} during the current outburst. The increase in absolute flux of the MEC and absorption components is connected to the reduction of ionization during outburst. The meaning and reality of the pedestal and bump components are uncertain. CI Cyg moved for less than 29 per cent of its orbit during the time interval covered by the Hα profiles in Fig. 3. We plan to extend these high-resolution observations for at least a full orbital period before attempting any detailed modelling.

ACKNOWLEDGMENT

We would like to thank P. Ochner for his assistance with some of the observations discussed here.

REFERENCES

Belyakina T. S., 1979, Izv. Krym. Astrofiz. Obs., 59, 133
Belyakina T. S., 1984, Izv. Krym. Astrofiz. Obs., 68 108
Drilling J. S., Landolt A. U., 2000, in Cox A. N., ed., Allen's Astrophysical Quantities. Springer, New York, p. 381
Fekel F. C., Joyce R. R., Hinkle K. H., Skrutskie M. F., 2000, AJ, 119, 1375 (F00)
Godon P., 1996, AJ, 462, 456
Henden A., Munari U., 2006, A&A, 458, 339
Henden A., Munari U., 2008, Baltic Astron., 17, 293
Kenyon S. J., 1986, The Symbiotic Stars. Cambridge Univ. Press, Cambridge (K86)
Kenyon S. J., Oliversen N. A., Mikołajewska J., Mikołajewski M., Stencel R. E., Garcia M. R., Anderson C. M., 1991, AJ, 101, 637 (K91)
Merrill P. W., Humason M. L., 1932, PASP, 44, 56
Mikołajewska J., 1997, in Mikołajewska J., ed., Physical Processes in Symiotic Binaries and Related Objects. Copernicus Foundation for Polish Astronomy, Warsaw, p. 3
Mikołajewska J., 2003, in Corradi R. L. M., Mikołajewska J., Mahoney T. J., eds, ASP Conf. Ser. Vol. 303, Symboitic Stars Probing Steller Evolution. Astron. Soc. Pac., San Francisco, p. 9
Mikołajewska J., Mikolajewski M., 1983, Acta Astron., 33, 403
Mikołajewska J., Kolotilov E. A., Shugarov S. Yu., Tatarnikova A. A., Yudin B. F., 2003, in Corradi R. L. M., Mikołajewska J., Mahoney T. J., eds, ASP Conf. Ser. Vol. 303, Symbiotic Stars Probing Stellar Evolution. Astron. Soc. Pac., San Francisco, p. 151
Munari U., Buson L. M., 1994, A&A, 287, 87
Munari U., Yudin B. F., Kolotilov E. A., Gilmore A. C., 1995, AJ, 109, 1740
Munari U., Siviero A., Cherini G., Tomaselli S., Graziani M., Tozzi F., Moretti S., 2008, Central Bureau Electronic Telegram, 1487
Mürset U., Schmid H. M., 1999, A&AS, 137, 473
Paczynski R., Rudak R., 1980, A&A, 82, 349
Shapley H., 1922, Harvard College Obs. Bull., 778, 2
Sokoloski J. L., 2003, in Corradi R. L. M., Mikołajewska J., Mahoney T. J., eds, ASP Conf. Ser. Vol. 303, Symboitic Stars Probing Stellar Evolution. Astron. Soc. Pac., San Francisco, p. 202
Sokoloski J. L. et al., 2006, ApJ, 636, 1002
Sowell J. R., Trippe M., Caballero-Nieves S. M., Houk N., 2007, AJ, 134, 1089
Straižys, V. 1992, Multicolor Stellar Photometry. Pachart Publishing House, Tucson
Tutukov A. V., Yungelson L. R., 1976, Astrofizika, 12, 521
van der Bergh S., Younger P. F., 1987, A&AS, 70, 125
Warner B., 1995, Cataclysmic Variable Stars. Cambridge Univ. Press, Cambridge

This paper has been typeset from a TEX/LATEX file prepared by the author.